IUST
Iran University of Science and Technology

Iranian Journal of Electrical and Electronic Engineering

Journal Homepage: ijeee.iust.ac.ir

Research Paper

Design and Optimizing of a GaN HEMT Power Amplifier Based on the Inclined Planes System Optimization Algorithm for Wireless Applications

M. Soruri*, S. M. Razavi*(C.A.), and M. Forouzanfar*

Abstract: Power amplifier is one of the main components in the RF transmitters. It must provide various stringent features that can lead to complicating the design. In this paper, a new optimizing method based on the inclined planes system optimization algorithm is presented for the design of a discrete power amplifier. It is evaluated in a 2.4-3 GHz power amplifier, which is designed based on "Cree's CGH40010F GaN HEMT". The optimization goals are input and output return losses, Power Added Efficiency, and Gain. Large signal simulation of the optimized power amplifier shows a good performance across the bandwidth. In this frequency range, the input and output return losses are about lower than -10 dB, the Power Added Efficiency is greater than 51%, while the Gain is higher than 13.5 dB. A two-tone test with a frequency space of 1 MHz is applied for the linearity evaluation of the designed power amplifier. The obtained result shows that the power amplifier has good linearity with a low memory effect.

Keywords: Gain, Inclined Planes System Optimization, Optimization, Power Added Efficiency, Power Amplifier.

1 Introduction

POWER amplifier (PA) design is one of the most important issues in the designing of the RF transmitter. Recently, various designs and structures have been presented to enhance the power amplifier's performance. Since the power amplifiers are the final stage of the transmitters, it drives with a large input signal, which makes nonlinearity in the amplifier characteristic. In addition, it works under high current and voltage conditions, which can create a high power consumption. Therefore, the power amplifier characteristic can affect the overall linearity and efficiency of a transmitter. As a result, the high efficiency and sufficient linearity become two challenging issues in the power amplifier design, which cannot easily be met simultaneously.

The power amplifier can be implemented in different technologies [1]. Monolithic Microwave Integrated Circuits (MMIC) have been extensively used due to their excellent repeatability, small size, and high integration capability [2]. Despite all these features, their fabrication process is expensive, and they are not suitable for high-power applications [3]. Another technology is the Quasi-Monolithic Integrated Technology (QMIT), which provides adequate frequency response and good thermal behavior, but thin-film technologies are required for realization [4]. A discrete power amplifier is another type of power amplifier implementation. It can be easily realized based on the inexpensive substrate with appropriate thermal characteristics. Also, they are suitable for high-power applications. However, the bandwidth can be limited due to the high parasitics of their inter-connections [5].

The power amplifier's characteristics are highly dependent on the amplifier's bias current and operating mode [6, 7]. In the bias current classification, power amplifiers are divided into four classes: A, AB, B, and C, and in operating mode classification, power

Iranian Journal of Electrical and Electronic Engineering, 2022.
Paper first received 07 December 2021, revised 14 April 2022, and accepted 23 April 2022.
* The authors are with the Faculty of Electrical and Computer Engineering, University of Birjand, Birjand, Iran.
E-mails: mohamad.soruri@birjand.ac.ir, smrazavi@birjand.ac.ir, and forouzanfar@birjand.ac.ir.
Corresponding Author: S. M. Razavi.
https://doi.org/10.22068/IJEEE.18.3.2369

amplifiers are divided into two categories [6]: switched-mode such as class D, E, G, H, and current mode PA such as Class F, Class 2nd HT and Class 2nd & 3rd Harmonic Terminations (HT). In each of these categories and classes, linearity and efficiency are challenging each other. Due to the new applications of power amplifiers in low power consumption systems, the design of a power amplifier with sufficiently high efficiency and an appropriate power gain is a critical issue [8]. Therefore, the input and output matching network should be carefully designed and implemented to achieve the power amplifier's best performance. In power amplifier design, consideration of the large-signal analysis of selected transistors via load-pull simulation is necessary [9].

Recently, using the evolutionary algorithms for multi-objective optimization in the VLSI circuits design have been widely used [10, 11]. Design and optimization of a CMOS power amplifier using innovative fractional-order Particle Swarm Optimization (PSO) have been considered by Hosseini *et al.* in [12] and in the design of 2.4 GHz PA for wireless applications. Optimization of operational transconductance amplifiers by the evolutionary algorithm and gm/ID method has been studied in [13]. In [14], the PSO algorithm is used for designing a pre-distorter to increase the linearity of a power amplifier. In [11], the power amplifier parameters are optimized for achieving an acceptable result at 2.4 GHz for Wireless Personal Area Network (WPAN). Annealing simulation with PSO algorithm carried out in [15] for designing a high-efficiency 10W power amplifier. LDMOS modeling and a high-efficiency power amplifier design were worked on by Jahanbakht *et al.* in [16] for achieving a better Power Added Efficiency (PAE) and a high Gain. A linearization technique for improving power amplifier performance is suggested in [17] with the PSO algorithm and Artificial Bee Colony (ABC) algorithm. An automated power amplifier design using the PSO algorithm is introduced by Peng *et al.* in [18], which is used for the design of a 2.14 GHz high PAE power amplifier.

In this paper, a broadband 10W GaN HEMT power amplifier optimized with the Inclined Planes system Optimization (IPO) algorithm is presented. IPO is an optimization algorithm that was first introduced by Mozaffari *et al.* in 2016 [19]. In this approach, at first, the widths and lengths of the microstrip lines in the RF section of the amplifier are manually tuned to get the best possible result, then these obtained values of the variables are defined as a leading point of the search space of the IPO and algorithm is applied for obtaining the best result. For a specified iteration value, the algorithm converges to the defined and desired values. The rest of the paper is organized as follows: the proposed algorithm is introduced in Section 2. In Section 3, the IPO algorithm and method of its implementation for power amplifier design are described. Section 4, shows how the parameters of the proposed amplifier were optimized. In Section 5, simulation results are shown, and finally, in Section 6, conclusion and future work are presented.

2 Proposed Algorithm

Fig. 1 shows the overall block diagram of the proposed algorithm. As described in the block diagram, we first manually tuned the parameters of the PA to find the optimum value for the leader particle. To find this point, we first should perform the load-pull simulation to find the best input and output terminations. Then, we tune the widths and lengths of the stubs of the PA to satisfy the required feature in all frequency ranges. After finding the best value for the leader particle, we apply the IPO algorithm to find the optimum values of widths and lengths.

For applying the optimization algorithm, at first, we should define our fitness function. The efficiency of PA is one of the fitness functions that should be optimized, which is defined as follows [20]:

$$\eta_D = \frac{P_o}{P_{DC}} \tag{1}$$

where in (1), η_D is the drain efficiency and P_o and P_{DC} are the output power and total power consumption, respectively. According to another definition of efficiency (η_D) [6], we can relate the efficiency to the dissipation power in the transistor, which is expressed in (2).

$$\eta_D = \frac{P_{out,f}}{P_{DC}} = \frac{P_{out,f}}{P_{diss} + P_{out,f} + \sum_{n=2}^{\infty} P_{out,nf}} \tag{2}$$

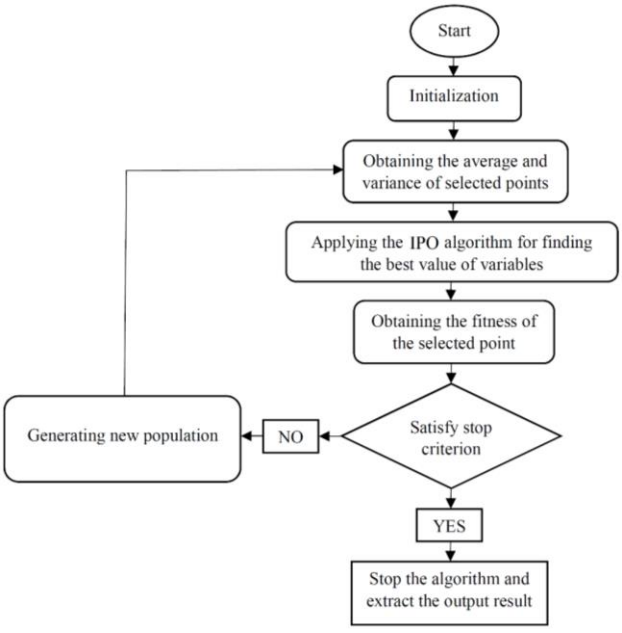

Fig. 1 Block diagram of the proposed algorithm.

where in (2), P_{diss} is the dissipation power in the transistor, $P_{out,f}$ is the output power in the fundamental frequency, while $\sum_{n=2}^{\infty} P_{out,nf}$ shows the sum of the output powers in the harmonic frequencies. If we want to achieve the highest efficiency, we should minimize P_{diss} and $\sum_{n=2}^{\infty} P_{out,nf}$. In other words, the highest efficiency is available (η_D = 100), if and only if the following equations are satisfied.

$$P_{diss} = \frac{1}{T}\int_0^T v_{DS}(t).i_D(t)\,dt = 0 \tag{3}$$

$$\begin{aligned}\sum_{n=2}^{\infty} P_{out,nf} &= \frac{1}{2}\sum_{n=2}^{\infty} V_n I_n \cos(\phi_n) \\ &= \frac{1}{2}\sum_{n=2}^{\infty} Z_n I_n^2 \cos(\phi_n) \\ &= \frac{1}{2}\sum_{n=2}^{\infty} Y_n V_n^2 \cos(\phi_n) = 0\end{aligned} \tag{4}$$

Equation (3) refers to the fact that there should be no overlap between drain voltage and current waveforms to maximize efficiency. Equation (4) expresses that the output power must be zero in each harmonic frequency. We use (3) and (4) to minimize the power amplifier's dissipation power and thus, maximize the efficiency.

PAE is another definition of efficiency that provides a more precise definition for efficiency that becomes dependent on the input power P_{in}. PAE is defined as follows [20]:

$$PAE = \frac{P_o - P_{in}}{P_{DC}} \tag{5}$$

where in (5), P_{in} is the input power. Another fitness function is the Gain, which is defined as follows [20]:

$$G = \frac{P_o}{P_{in}} \tag{6}$$

Two other cost functions are the Input Return Loss (RL_In) and Output Return Loss (RL_Out) which determine the power loss rate in the PA's input and output, respectively. The lower values of these two parameters mean better matching and thus lower loss. In the proposed PA optimization algorithm, the above equations were used as our cost functions.

3 IPO Algorithm

The method of optimizing the IPO is inspired by the dynamic movement of spherical objects on the friction-free sloping surface, all of which interact to reach the lowest point of the surface. In IPO, a numeral of small balls seeks the search area to meet the optimal point. The original idea of the algorithm is the height relative to a reference point per ball, which is gained based on the fitness function [19, 21, 22]. Every ball in the research space has three peculiarities: position, height, and angle that it makes with other balls.

Balls in our optimization algorithm, are the values of the widths and lengths of the microstrip lines in the PA that are generated randomly at the beginning of the algorithm. Each particle in the search space can be represented by a vector of 16 values. Therefore, each particle has 16 dimensions. The vector parameters of the particles are defined as follows (The unit of parameters is in millimeters):

$$\begin{aligned}p = \big[&W_{i_1}, L_{i_1}, W_{i_2}, L_{i_2}, W_{i_3}, L_{i_3}, W_{d_1}, L_{d_1}, \\ &W_{d_2}, L_{d_2}, W_{o_1}, L_{o_1}, W_{o_2}, L_{o_2}, W_{o_3}, L_{o_3}\big]\end{aligned} \tag{7}$$

where W_{i_1}, L_{i_1}, W_{i_2}, L_{i_2}, W_{i_3}, and L_{i_3} are the widths and lengths of the input matching network, W_{d_1}, L_{d_1}, W_{d_2}, and L_{d_2} are the widths and lengths of the drain and W_{o_1}, L_{o_1}, W_{o_2}, L_{o_2}, W_{o_3}, and L_{o_3} are the output matching network. It is necessary to mention this point that before using the IPO algorithm, a manual tune is performed to obtain the best initial result. Then, this initial result is considered as a leader point in the search space so the best position of the particles is obtained according to this point.

4 Optimizing of PA Parameters With IPO Algorithm

Fig. 2 shows the schematics of the proposed PA in ADS software. As mentioned in the previous section, particles are the values of the widths and lengths of the stubs in the drain/gate pads and the input and output matching network. For evaluating the fitness of each particle, we should compute RL_In, RL_Out, *PAE*, and the Gain of the PA. In the proposed circuit, we have used a parallel resistor and capacitor in the transistor gate to stabilize the PA.

Table 1 shows the range of widths and lengths of the microstrip lines that should optimize with the IPO algorithm. The lower and upper bounds of parameters in this table are chosen based on the values obtained in the manual tuning. Table 2 shows the minimum or maximum requirement values of the objective function that should satisfy the design parameters. By performing a manual tuning, the leader point specification, which are the corresponding values of the parameters of the vector *p* in (7), are as follows:

$$\begin{aligned}p_{leader} = \big[&0.94 \quad 20.58 \quad 0.57 \quad 6.08 \quad 1 \quad 7.86 \quad 8.37 \quad 12 \\ &10.4 \quad 2.32 \quad 7.05 \quad 7.85 \quad 12 \quad 1.04 \quad 47.2 \quad 0.13\big]\end{aligned}$$

As is said, the values in p_{leader} vector, are in millimeters. The optimization algorithm is performed based on the following steps:

Step 1: Initializing the population (a vector with 16 variables).

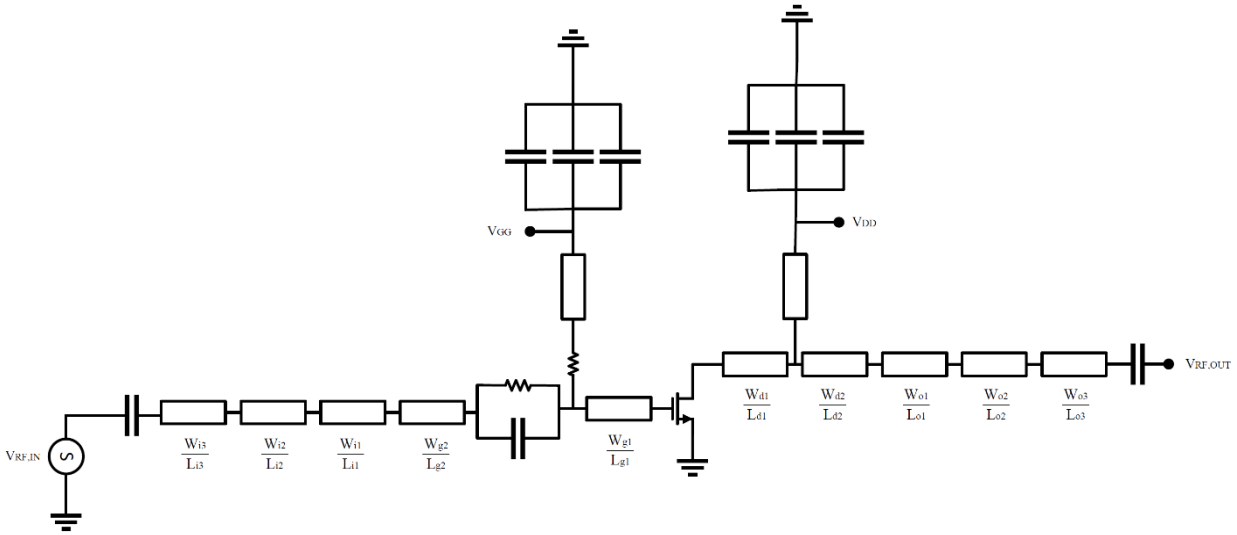

Fig. 2 Schematics of the proposed PA.

Table 1 PA parameters and their value range in the IPO algorithm.

Parameter	W_{i_1}	L_{i_1}	W_{i_2}	L_{i_2}	W_{i_3}	L_{i_3}	W_{d_1}	L_{d_1}	W_{d_2}	L_{d_2}	W_{o_1}	L_{o_1}	W_{o_2}	L_{o_2}	W_{o_3}	L_{o_3}
Lower bound	0.05	11	0.2	6	1	5	0.5	0.5	0.5	0.5	0.5	1	1	0.5	12	0.1
Upper bound	10	25	5	15	10	11	8	8	15	15	12	15	9	8	50	4

Table 2 Objective function and the range of desired value.

Objective function	The range of desired value
RL_Out	<-10dBm
RL_In	<-10dBm
PAE	>50%
Gain	>13.5dB

Step 2: Obtaining the 601 points with a distance of 1 MHz in the bandwidth range and their average and variance values.
Step 3: Evaluation of each particle based on the defined fitness function (RL_In, RL_Out, *PAE*, and Gain).
Step 4: Definition of an error function for each fitness function.
Step 5: return to step 2 until the condition is not met.
To achieve a flat Gain and *PAE* in the whole bandwidth region, we define a variance criterion. It can avoid the generation of large variations between the output results of the IPO algorithm [23].

$$\sigma^2 = \frac{1}{n}\sum_{i=1}^{n}(X_i - \overline{X})^2 \tag{8}$$

$$\overline{X} = \frac{x_1 + x_2 + x_3 + \ldots + x_n}{n} = \frac{\sum_{i=1}^{n} x_i}{n} \tag{9}$$

where in (9), $\overline{X}$ is the average of the 601 selected points. By applying (8) in the proposed algorithm, we can achieve the desired results with low variance.

5 Results

The proposed optimization algorithm was implemented in MATLAB software. For the implementation of the algorithm, we linked MATLAB to ADS during the optimization algorithm [24, 25]. The optimization algorithm is performed to find the best vectors of variables and dedicated cost function values for each. By considering the best values of the output result and considering a trade-off between the 4 defined cost functions, the best results are specified. Then, the best results are performed in the schematics of the circuit in the ADS algorithm, and the Harmonic Balance is carried out. Cree's CGH40010F GaN HEMT is the active device in the proposed circuit as shown in Fig. 2. The class of transistor biasing is deep AB, with I_D = 161 mA, V_{GS} = –2.7 V and V_{DD} = 28 V. The input frequency is swept from 2.4 GHz to 3 GHz with a 1 MHz frequency step.

It should be noted all high-frequency simulations of the proposed PA are performed using the precise non-linear model of the transistor, which is provided by Cree company. It is a non-linear model in which all non-linear effects, including non-linear capacitors of the transistor, non-linear transistor transconductance, and trapping/thermal-induced current dispersion, are accurately modeled. Therefore, all non-linear effects are considered in the simulations.

To increase the accuracy of the simulations, all high-frequency simulations have been performed in the momentum microwave environment of ADS software. The meshing frequency is 5 GHz, and at each stage of optimization, all transmission lines (including bias circuits) are meshed and simulated in the momentum microwave environment.

Table 3 shows the final optimized length and width

Table 3 The final optimized length and width values of the transmission lines.

Parameter	W_{i_1}	L_{i_1}	W_{i_2}	L_{i_2}	W_{i_3}	L_{i_3}	W_{d_1}	L_{d_1}	W_{d_2}	L_{d_2}	W_{o_1}	L_{o_1}	W_{o_2}	L_{o_2}	W_{o_3}	L_{o_3}
Value	2	14	1.5	13.89	8.73	6.39	0.8	1.2	13	8	10	14.63	7.27	7.43	14.5	2

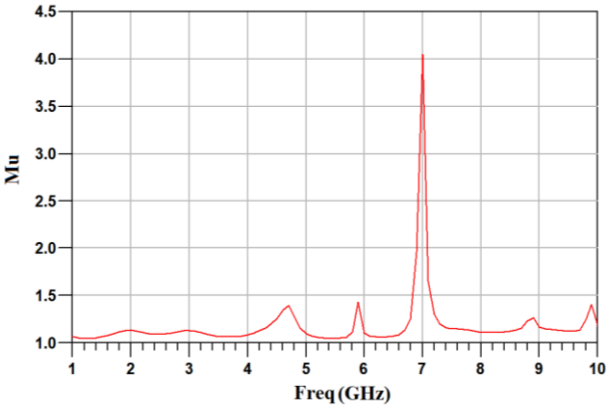

Fig. 3 The Mu factor of the optimized PA.

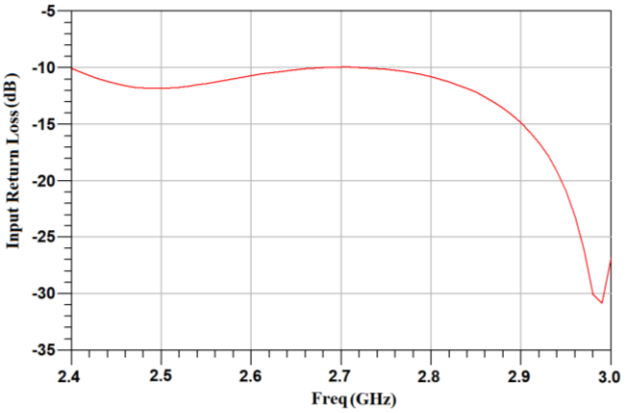

Fig. 4 Input Return Loss (RL_In) of the proposed PA.

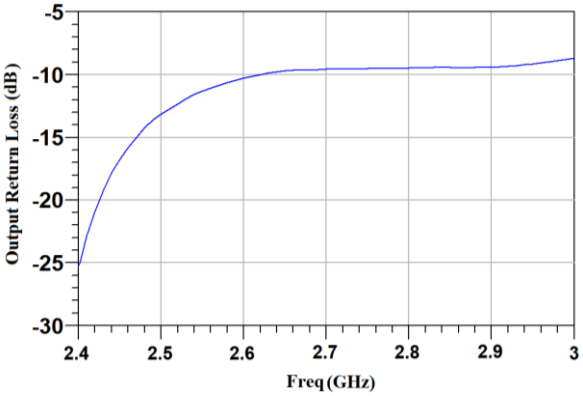

Fig. 5 Output Return Loss (RL_Out) of the proposed PA.

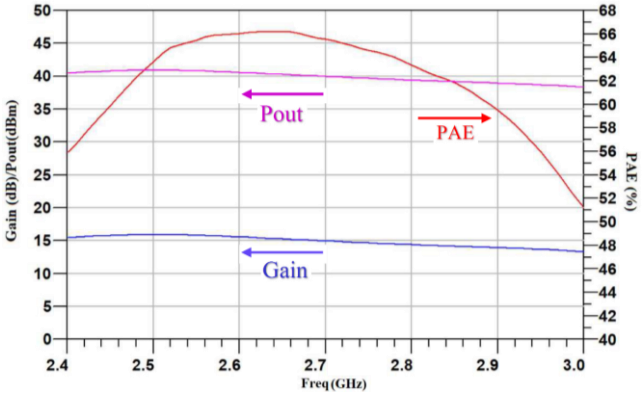

Fig. 6 Gain, *PAE*, and P_{out} of the proposed PA versus frequency.

values of the transmission lines after optimizing by the IPO algorithm. All values are in millimeters.

As is said, in the proposed circuit, we have used a parallel resistor and capacitor in the transistor gate to stabilize the PA. Before starting the optimization, suitable values for the capacitor and the resistance were selected in such a way as to stabilize the PA at all frequencies while PA can provide sufficient gain. The values of the selected resistor and capacitor were not among the optimization parameters. After optimizing the lengths and widths of all transmission lines, the stability parameter of the amplifier, that is Mu factor, was simulated, as shown in Fig. 3. The simulation results show that the amplifier is stable at all frequencies.

Figs. 4 and 5 show the value of the RL_In and RL_Out of the optimized PA, respectively. Based on the obtained values, RL_In is under the –10 dB, and RL_Out is lower than –9 dB in the frequency range of 2.4–3 GHz.

Fig. 6 shows P_{out}, *PAE*, and Gain of the proposed PA versus frequency. As Fig. 6 shows, *PAE* is above 51% in the desired frequency band. Also, the Gain is higher than 15 dB in the frequency range of 2.4 GHz to 2.7 GHz and is above the 13.5 dB in the whole bandwidth range. The PA provides an output power of 40 dBm, a Gain of 15 dB, and a *PAE* of 65% at the frequency of 2.7 GHz.

P_{out}, *PAE*, and Gain versus P_{in} at the frequency of 2.7 GHz are shown in Fig. 7. As shown in Fig. 7, the proposed PA provides a high *PAE*, an appropriate Gain, and sufficient output power due to applying the good optimization algorithm and obtaining the best values for the widths and lengths of the matching network in the proposed PA. Fig. 8 shows the fundamental and third harmonic output power versus P_{in} at the frequency of 2.7 GHz.

Fig. 9 shows IMD3 and IMD5 (high and low) versus P_{out} 2 tone. A two-tone test with a frequency space of 1 MHz was applied at a center frequency of 2.7 GHz for linearity evaluation of the designed power amplifier. Low IMD3 and low IMD5 are specified by red color and high IMD3 and high IMD5 are specified by blue color. Since for both IMD3 and IMD5, red and blue curves are completely on top of each other, the proposed PA has a good response for the time and thermal

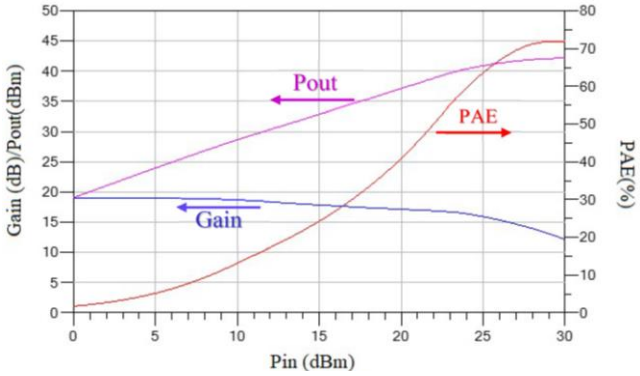

Fig. 7 Gain, *PAE*, and P_{out} of the proposed PA at the frequency of 2.7 GHz versus P_{in}.

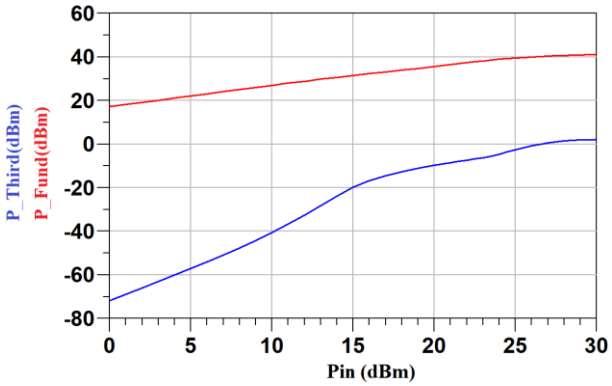

Fig. 8 Fundamental power and Third harmonic power at the frequency of 2.7 GHz versus P_{in}.

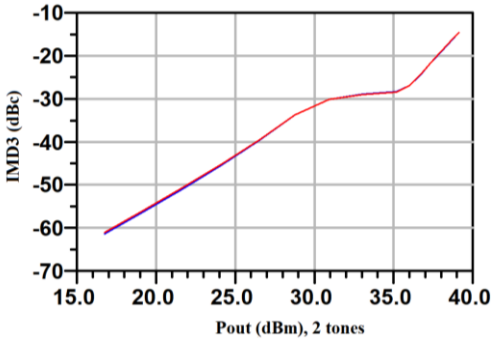

(a)

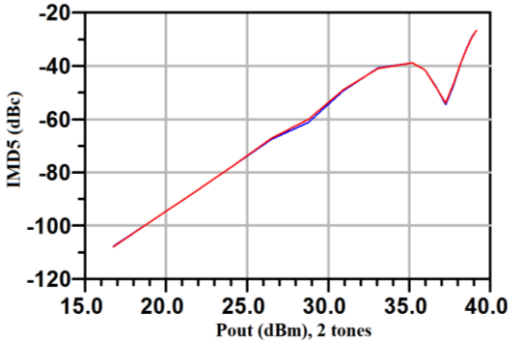

(b)

Fig. 9 IMD3 and IMD5 (low and high) versus P_{out}: a) IMD3 and b) IMD5.

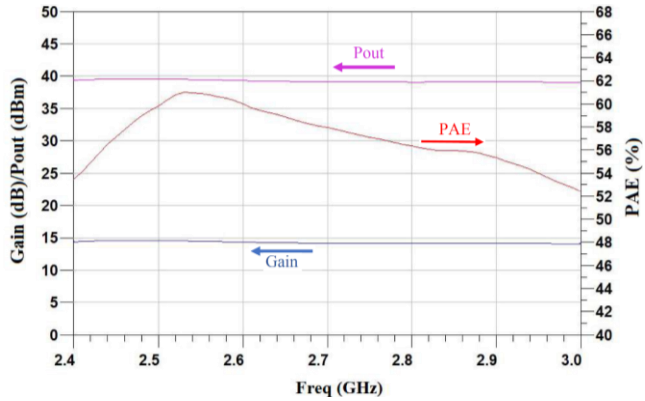

Fig. 10 Gain, *PAE*, and P_{out} of the proposed PA versus frequency in PA optimized by ADS optimizer.

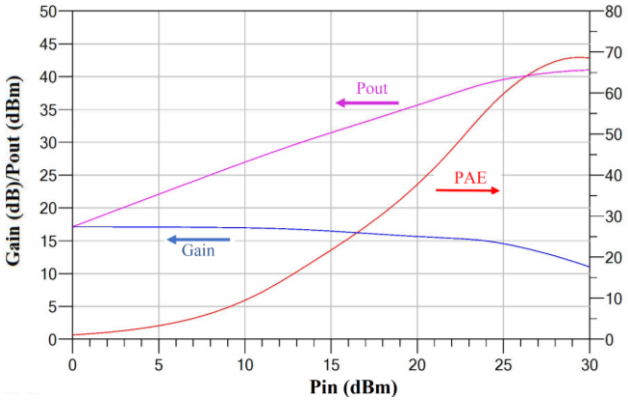

Fig. 11 Gain, *PAE*, and P_{out} of the proposed PA at the frequency of 2.7 GHz versus P_{in} in PA optimized by ADS optimizer.

variations and has a low memory effect.

For verifying our algorithm, we optimize the PA with the ADS gradient optimizer with the definition of the P_{out}, *PAE*, and Gain as the main goals. The results are shown in Fig. 10.

By comparing the result of optimizing PA with ADS optimizer and the proposed method in Figs. 10 and 6, respectively, we can see that the average of *PAE*, P_{out} and Gain in Fig. 6 is higher than Fig. 10. Also, *PAE* with the proposed method is above 62% in the frequency range of 2.44 GHz to 2.82 GHz, but *PAE* with the ADS optimizer is lower than 61% in the whole bandwidth range. P_{out} with the proposed method is above the 40dBm in the frequency range of 2.4 GHz to 2.7 GHz, but with the ADS optimizer is lower than 40 dBm in the whole bandwidth range. We can see similar behavior in Gain. With the proposed method, Gain is above 15 dB in the frequency range of 2.4 GHz to 2.7 GHz, but with the ADS optimizer is lower than 15 dB in the whole bandwidth range.

Fig. 11 shows P_{out}, *PAE*, and Gain versus P_{in} at the frequency of 2.7 GHz for PA optimized with the ADS gradient optimizer. As mentioned, Fig. 7 is the obtained results with PA optimized by the IPO algorithm. Carefully in the results shown in Figs. 7 and 11, we can conclude these points:

Table 4 Comparison of the proposed PA with some other proposed S-band Pas.

Ref.	[8]	[26]	[9]	[27]	[7]	[28]	[29]	[30]	This work
Frequency [GHz]	2-4	1.9-2.9	2-3	1.85 - 2.7	2.3-2.7	1.65-2.75	2.7-3.2	1-2.5	2.4-3
Gain [dB]	12.3-14.1	10-12.5	11.5-12.5	11	12	Not reported	10	12.3-14.1	13.5-15.9
PAE [%]	36.5-53.4	37-69	58-72	68-77 (DE)	57-66	55-72 (DE)	47	48-55	52-69
VDD [V]	28	28	28	Not reported	Not reported	47	28	28	28
P_{out}	10	10	10	10	10	Not reported	10	10	10

1. In the saturation region, where the input power is between 25 dBm and 30 dBm, *PAE* obtained with the proposed method is higher than *PAE* obtained with the ADS optimizer and has reached 70%, while *PAE* obtained with the ADS optimizer is lower than 70%.
2. In the saturation region, P_{out} obtained with the ADS optimizer is higher than about 39 dBm, while P_{out} obtained with the proposed method is higher than about 42 dBm.
3. The degradation of the Gain obtained with the ADS optimizer is slightly greater than the similar value obtained with the proposed method in the saturation region.

Table 4 summarizes the performance of some previously published S-band PA and compares their results with the proposed PA. As we can see, our proposed PA has a better performance in comparison with other works. We can see this performance improvement in the *PAE* and Gain of the PA.

6 Conclusion and Future Work

This paper described the optimization of a PA with an IPO algorithm, while a GaN HEMT that formed PA was designed based on this optimization algorithm. In the proposed optimization algorithm, the widths and lengths of microstrip lines are optimized in such a way as to minimize the return losses and power dissipation and thus increase the PA's efficiency and increase the power gain simultaneously. The optimized PA simulation result showed that the proposed algorithm could improve the *PAE* and Gain of PA. In the future, optimizing the parameters of the proposed PA will perform with other evolutionary algorithms.

Intellectual Property

The authors confirm that they have given due consideration to the protection of intellectual property associated with this work and that there are no impediments to publication, including the timing of publication, with respect to intellectual property.

Funding

No funding was received for this work.

CRediT Authorship Contribution Statement

M. Soruri: Idea & conceptualization, Research & investigation, Original draft preparation, Software and simulation. **S. M. Razavi:** Data curation, Analysis, Project administration, Supervision. **M. Forouzanfar**: Verification, Revise & editing, Software and simulation, Methodology.

Declaration of Competing Interest

The authors hereby confirm that the submitted manuscript is an original work and has not been published so far, is not under consideration for publication by any other journal and will not be submitted to any other journal until the decision will be made by this journal. All authors have approved the manuscript and agree with its submission to "Iranian Journal of Electrical and Electronic Engineering".

References

[1] M. Forouzanfar and M. Joodaki, "Systematic design of hybrid high power microwave amplifiers using large gate periphery GaN HEMTs," *AEU-International Journal of Electronics and Communications*, Vol. 84, pp. 225–233, 2018.

[2] J. Javidan and S. M. Atarodi, "Implementation of a fully integrated 30-dBm RF CMOS linear power amplifier with power combiner," *AEU-International Journal of Electronics and Communications*, Vol. 65, No. 6, pp. 502–509, 2011.

[3] B. Kim, M. Greene, and M. Osmus, "Broadband high efficiency GaN discrete and MMIC power amplifiers over 30–2700 MHz range," in *IEEE MTT-S International Microwave Symposium (IMS2014)*, pp. 1–3, Jun. 2014.

[4] M. Joodaki, G. Kompa, and H. Hillmer, "An enhanced quasi-monolithic integration technology for microwave and millimeter wave applications," *IEEE Transactions on Advanced Packaging*, Vol. 26, No. 4, pp. 402–409, 2003.

[5] P. Saad, H. M. Nemati, K. Andersson, and C. Fager, "Highly efficient GaN-HEMT power amplifiers at 3.5 GHz and 5.5 GHz," in *IEEE WAMICON 2011 Conference Proceedings*, 2011.

[6] P. Colantonio, F. Giannini, and E. Limiti, *High efficiency RF and microwave solid state power amplifier*. John Wiley & Sons, 2009.

[7] N. Tuffy, A. Zhu, and T. J. Brazil, "Class-J RF power amplifier with wideband harmonic suppression," in *IEEE MTT-S International Microwave Symposium*, pp. 1–4, 2011.

[8] X. Ding, S. He, F. You, S. Xie, and Z. Hu, "2–4 GHz wideband power amplifier with ultra-flat gain and high PAE," *Electronics Letters*, Vol. 49 No 5, pp. 326–327, 2013.

[9] X. Meng, C. Yu, Y. Liu, and Y. Wu, "Design approach for implementation of class-J broadband power amplifiers using synthesized band-pass and low-pass matching topology," *IEEE Transactions on Microwave Theory and Techniques*, Vol. 65, No. 12, pp. 4984–4996, 2017.

[10] M. Bhuvaneswari, *Application of evolutionary algorithms for multi-objective optimization in VLSI and embedded systems*. Springer, 2014.

[11] S. Manjula and D. Selvathi, "Design and optimization of ultra low power low noise amplifier using particle swarm optimization," *Indian Journal of Science and Technology*, Vol. 8, No. 36, pp. 1–8, 2015.

[12] S. A. Hosseini, A. Hajipour, and H. Tavakoli, "Design and optimization of a CMOS power amplifier using innovative fractional-order particle swarm optimization," *Applied Soft Computing*, Vol. 85, p. 105831, 2019.

[13] E. Tlelo-Cuautle and A. Sanabria-Borbon, "Optimising operational amplifiers by evolutionary algorithms and gm/Id method," *International Journal of Electronics*, Vol. 103, No. 10, pp. 1665–1684, 2016.

[14] G. Karimi and A. Lotfi, "An analog/digital pre-distorter using particle swarm optimization for RF power amplifiers," *AEU-International Journal of Electronics and Communications*, Vol. 67, No. 8, pp. 723–728, 2013.

[15] C. C. Li, F. You, T. Yao, J. Wang, W. Shi, J. Peng, and S. He, "Simulated annealing particle swarm optimization for high-efficiency power amplifier design," *IEEE Transactions on Microwave Theory and Techniques*, Vol. 69, pp. 2494–2505, 2021.

[16] M. Jahanbakht and M. T. Aghmyoni, "Ldmos modeling and high efficiency power amplifier design using PSO algorithm," *Progress In Electromagnetics Research M*, Vol. 27, pp. 219–229, 2012.

[17] P. Bipin and P. Rao, "Linearization of high power amplifier using modified artificial bee colony and particle swarm optimization algorithm," *Procedia Technology*, Vol. 25, pp. 28–35, 2016.

[18] P. Chen, S. He, and F. You, "Automated power amplifier design assisted with particle swarm optimization," in *IEEE Asia Pacific Microwave Conference Proceedings*, pp. 481–483, 2012.

[19] M. H. Mozaffari, H. Abdy, and S. H. Zahiri, "IPO: An inclined planes system optimization algorithm," *Computing and Informatics*, Vol. 35, No. 1, pp. 222–240, 2016.

[20] I. Bahl, *Fundamentals of RF and microwave transistor amplifiers*. John Wiley & Sons, 2009.

[21] A. Mohammadi and S. H. Zahiri, "Inclined planes system optimization algorithm for IIR system identification," *International Journal of Machine Learning and Cybernetics*, Vol. 9, No. 3, pp. 541–558, 2018.

[22] S. Zandian, H. Khosravi, and A. Bijari, "Design and heuristic optimization of a CMOS LNA for ultra-wideband receivers," in *IEEE 27th Iranian Conference on Electrical Engineering (ICEE)*, 2019.

[23] D. C. Montgomery and G. C. Runger, *Applied statistics and probability for engineers*. John Wiley & Sons, 2010.

[24] https://www.mathworks.com/matlabcentral/fileexchange/76183-keysight-advanced-design-system-ads-to-matlab-interface.

[25] https://github.com/korvin011/ADS-Matlab-Interface

[26] Q. H. Le, C. T. Nghe, and G. Zimmer, "High efficiency 10 W GaN-HEMT power amplifier with optimum input stabilization," in *IEEE International Conference on Advanced Technologies for Communications (ATC)*, pp. 27–30, 2017.

[27] A. S. Sayed and H. N. Ahmed, "A 10-W, high efficiency, broadband harmonically tuned GaN-HEMT power amplifier," in *IEEE International Symposium on Circuits and Systems (ISCAS)*, pp. 1–4, 2018.

[28] R. Ma, S. Goswami, K. Yamanaka, Y. Komatsuzaki, and A. Ohta, "A 40-dBm high voltage broadband GaN Class-J power amplifier for PoE micro-basestations," in *IEEE MTT-S International Microwave Symposium Digest (MTT)*, pp. 1–3, 2013.

[29] U. Goyal, S. K. Tomar, M. Mishra, and S. Vinayak, "Design and development of S band 10W And 20W power amplifier," in *IEEE Applied Electromagnetics Conference (AEMC)*, pp. 1–2, 2015.

[30] A. E. Mahdi, A. G. Sobih, and M. A. El-Kafafi, "Design and implementation of 10W, highly linear, wideband and efficient power amplifier using harmonic termination," in *IEEE Middle East Conference on Antennas and Propagation (MECAP)*, pp. 1–4, 2016.

M. Soruri received the B.Sc. degree from the University of Shahid Bahonar, Kerman, Iran, in 2009, and the M.Sc. degree in Electronic Engineering from the University of Birjand, Birjand, Iran, in 2012, where he is currently pursuing the Ph.D. degree in Electronic Engineering. In 2021, he spent an exchange period at the University of Rome "Tor Vergata,"' Italy, as a Visiting Researcher. His current research interests include RF power amplifiers, low noise amplifiers (LNA), and machine learning algorithms.

S. M. Razavi received the B.Sc., M.Sc., and Ph.D. degrees in Electrical Engineering from the Amirkabir University of Technology and Tarbiat Modares University in 1994, 1996, and 2006, respectively. He is currently an Associate Professor at the University of Birjand, Birjand, Iran. His research interests include intelligent systems, pattern recognition, handwriting recognition, and analysis of RF microwave circuits.

M. Forouzanfar received the BS, MS, and Ph.D. degrees in electrical engineering from the Ferdowsi University of Mashhad in 2006, 2009, and 2017 respectively. He is currently an assistant professor at the University of Birjand, Birjand, Iran. His research interests include modeling, design, and analysis of RF microwave circuits.